Determining the number of layers in few-layer graphene by combining Raman spectroscopy and optical contrast

Bayle, Maxime; Reckinger, Nicolas; Felten, Alexandre; Landois, Périne; Lancry, Ophélie; Dutertre, Bertrand; Colomer, Jean François; Zahab, Ahmed Azmi; Henrard, Luc; Sauvajol, Jean Louis; Paillet, Matthieu

Published in:
Journal of Raman Spectroscopy

DOI:
10.1002/jrs.5279

Publication date:
2018

Document Version
Early version, also known as pre-print

Journal of RAMAN SPECTROSCOPY

Determining the number of layers in few-layer graphene by combining Raman spectroscopy and optical contrast

Journal:	*Journal of Raman Spectroscopy*
Manuscript ID	JRS-17-0186
Wiley - Manuscript type:	Research Article
Date Submitted by the Author:	29-Jun-2017
Complete List of Authors:	Bayle, Maxime; L2C Reckinger, Nicolas; Department of Physics and Research Group on Carbon Nanostructures (CARBONNAGe) Felten, Alexandre; Department of Physics and Research Group on Carbon Nanostructures (CARBONNAGe) Landois, Périne; L2C Lancry, Ophelie; HORIBA Jobin Yvon S.A.S. Dutertre, Bertrand; HORIBA Jobin Yvon S.A.S. Colomer, Jean-François; Department of Physics and Research Group on Carbon Nanostructures (CARBONNAGe) Zahab, Ahmed; L2C Henrard, Luc; Department of Physics and Research Group on Carbon Nanostructures (CARBONNAGe) Sauvajol, Jean-Louis; L2C Matthieu, Paillet; L2C
Keywords:	Graphene

Determining the number of layers in few-layer graphene by combining Raman spectroscopy and optical contrast

Maxime Bayle[1,*], Nicolas Reckinger[2], Alexandre Felten[2], Périne Landois[1], Ophélie Lancry[3], Bertrand Dutertre[3], Jean-François Colomer[2], Ahmed-Azmi Zahab[1], Luc Henrard[2], Jean-Louis Sauvajol[1] and Matthieu Paillet[1]

1 Laboratoire Charles Coulomb, CNRS-University of Montpellier, Place E. Bataillon, 34095 Montpellier, France

2 Department of Physics and Research Group on Carbon Nanostructures (CARBONNAGe), University of Namur, 61 rue de Bruxelles, 5000 Namur, Belgium

3 HORIBA Jobin Yvon S.A.S., 231 rue de Lille, 59650 Villeneuve d'Ascq

* Present address: Institut des Matériaux Jean Rouxel, UMR 6502 CNRS/Université de Nantes 2, rue de la Houssinière, BP 32229, 44322 Nantes Cedex 3, France.

Abstract

Raman spectroscopy is commonly used to determine the number of layers of few-layer graphene (FLG) samples. In this work, we focus on the criteria based on the G-band integrated intensity and on the laser optical contrast. Limitations due to stacking order are discussed and lead to the conclusion that it is necessary to combine Raman and optical contrast to avoid misinterpretation. Both methods enable to distinguish unambiguously between single layer graphene and multilayer graphene. However, neither each method separately nor the combination of the two enable a determination of the number of layers for all possible stacking orientations. Importantly, since the two methods always significantly disagree when they fail, the comparison of the values deduced by each method allows to discriminate if the determined number of layers can be specified or not. Other important parameters (substrate, laser wavelength, objective numerical aperture) are discussed to define a reliable method to determine the number of graphene layers in FLG and its domain of validity. The proposed method which combines Raman and optical contrast measurements, carried out with a 532 nm laser and using a 100x objective with a numerical aperture of 0.9, allows the determination of the number of layers for (up to 5) FLG on the following substrates: (i) glass (soda lime glass or similar with refractive index between 1.50 and 1.55) and (ii) oxidized silicon (SiO_2 on silicon, with a SiO_2 thickness of 90 ± 5 nm). The method is however limited to high quality graphene and FLG with small defect density and low residue.

1) Introduction

Graphene, a single-layer of carbon atoms arranged in a honeycomb lattice, has a high potential for future nanotechnology applications due to its excellent conductivity, transparency and flexibility [1]. Many physical properties of graphene and few layer graphene (FLG) depend on the number of layers. For example, monolayer and some FLG admit a linear dispersion relation of electronic bands and consequently show specific quantum Hall effect and conductivity [2,3]. Optical transparency and chemical activity are also related to the number of layers and their stacking order [4-6]. Therefore, the reliable identification of the layer number (N) of FLG flakes is essential to their fundamental study and the development of applications. Multilayer graphene flakes obtained by micro-mechanical cleavage of single-crystal graphite (SCG) or highly oriented pyrolytic graphite (HOPG) [7] retain the stacking structure of the bulk [8]. They are thus most often Bernal-stacked or show less commonly a rhombohedral-stacking structure [9]. Both kinds of structures correspond to commensurate multilayer stacks. However, for multilayer systems, many departures from these structures are observed including variations in interlayer distance, stacking faults and rotational mismatches [10,11]. The stacking structure influences the physical properties of multilayer graphene and it is thus crucial to take this parameter into account and to evaluate its impact on the methods used to count the number of layers.

Several optical methods have been used for counting the number of layers of 2D materials (for a recent review see Ref. [12]). Among the different techniques used, Raman spectroscopy is considered as an ideal tool (see Ref. [13] and references therein) to analyze and to study single layer graphene (1LG) and FLG (defined as in Ref. [14]) and is commonly used to determine the number of layers, but also their relative orientations, the crystalline quality and the effect of perturbations such as strain, doping, and disorder. More specifically, the dependence of the features of the Raman-active modes on the number of layers (N) has been studied in detail and several criteria have been proposed for N determination purpose. The first class of criteria rely on the wavenumbers and/or numbers of modes due to in-plane or out-of-plane relative motions of the layers (shear modes and layer breathing modes [15,16] or N modes [17]) and which are consequently absent in 1LG. Although these modes can be advantageously used for different purposes, their main disadvantages are their low intensity or their stacking/laser wavelength dependency or to require specific equipment for their measurement. But certainly the most problematic one is their absence in 1LG which makes the application of these criteria for 1LG identification questionable.

Another category of criteria relies on peaks, namely the G-band and 2D-band, observed in multilayer graphene as well as in 1LG. The full width at half maximum of the 2D-band (Γ_{2D}) and the ratio between 2D-band and G-band integrated intensity (A_{2D}/A_G) as a function of N have been commonly used in the literature as metrics to distinguish 1LG and FLG. It has been proposed that 1LG has the lowest Γ_{2D} and highest A_{2D}/A_G than FLG. As reported in ref. [18], none of these criteria hold true for all stacking order. Indeed, from the systematic investigation of a large number of flakes, we evidenced, in a previous paper [18], different and even opposite behaviors of both features with N. Our results were analyzed as the consequences of different stacking order between consecutive graphene layers. In agreement with

published reports on twisted bilayer graphene (2LG) [19-22], we have demonstrated that higher values of the A_{2D}/A_G ratio and narrower 2D bandwidths than those measured on 1LG can be measured on twisted FLG. In terms of control characteristics, these results confirm that neither A_{2D}/A_G nor Γ_{2D} are universal criteria to identify 1LG or to count the number of layers in FLG. The sensitivity of these quantities to doping or strain also impact their reliability [23-26]. As a consequence, criteria based on the 2D band suffer from several limitations.

The G-band area or integrated intensity (A_G) has been proposed as a criterion to count the number of graphene layers in FLG. In this paper, we examine in details the limitations or domain of validity of this criterion. It was found from experiments performed on exfoliated Bernal or rhombohedral stacked FLG (named AB-NLG, resp. ABC-NLG, in the following for N Layers Graphene) that A_G increases step by step with the number of layers [27-30]. Since it relies on Raman intensity measurement, it is necessary to define a reference for intensity normalization for the comparison of results obtained on different systems and in different laboratories. Silicon has been used as an intensity reference especially in the case of FLG deposited on SiO_2/Si substrates [31,32]. However, this procedure suffers from many drawbacks [12] which makes it hardly transferable and universal since the silicon peak intensity depends on several parameters like the excitation wavelength and polarization, its crystal orientation, the SiO_2 top layer thickness and the spectrometer/optical setup response since the Si Raman peak wavenumber is significantly different than the one of G-band. On the contrary, graphite (*i.e.* HOPG or SCG) is a more suitable intensity reference since its use requires no correction related to the sensitivity of the optical setup/spectrometer. Thus, we use the HOPG G-band area (A_G^{HOPG}) for intensity normalization. In the following, A_G^{Norm} stands for the ratio between A_G and A_G^{HOPG} measured in the exact same conditions. A_G^{Norm} has the advantage to enable to distinguish in all cases between 1LG and FLG, if the signal to noise ratio is high enough. However, regarding the FLG number of layers counting, two limitations related to the relative orientation and stacking of the graphene layers exist. First, an intensity enhancement occurs due to changes in the electronic joint density of states, for given relative orientations of the layers [33]. Second, a significant G-band intensity decrease (down to 70% of the one of equivalent Bernal stacked structures) has been reported for some relative layer orientations [34,35]. These two limitations circumvent the use of A_G alone as a metric for counting the number of layers.

To solve this problem, we propose that the simultaneous measurement of the optical contrast (OC) can be advantageously used as a complementary criterion. The OC in the visible range, defined by OC = (Rs-R)/Rs, where R (resp. Rs) is the reflected intensity of the light measured on each point of the sample (resp. on the bare substrate), has also been proposed as a tool for counting graphene layers [36-38]. Indeed, the optical properties of FLG are, in most cases, directly related to N. However, OC is also changing near optical resonances as reported for twisted 2LG [39]. In this case, this criterion alone will also lead to a wrong determination of the number of layers.

Moreover, both A_G and OC are strongly dependent on the nature of the substrate and on the used laser wavelength used [29,30,36,37,38,40]. This implies that each substrate needs to be specifically studied and a large set of experimental data is a necessary prerequisite to validate theoretical predictions.

In this paper, we propose a reliable method for the specification of the number of layers for FLG samples deposited on soda lime glass or SiO_2/Si substrates. This method is based on the combination of Raman spectroscopy (A_G^{Norm}) and OC. Both methods enable to distinguish unambiguously between 1LG and multilayer graphene. However, neither each method separately nor the combination of the two enable a determination of the number of layers for all possible stacking orientations. But importantly, since the two methods always significantly disagree when they fail, the comparison of the values deduced by each method allows to discriminate if the determined number of layers is correct and can be specified or not.

Our approach, combining simultaneous Raman spectroscopy and laser optical contrast (and extinction for transparent substrates) mapping, is first presented in the experimental section. This method enables to discuss the evolution of A_G and OC in FLG as briefly exemplified in the following section. Then, we discuss the limitations of the A_G and OC criteria related to the relative orientation and stacking of the graphene layers. We show that it is necessary to combine both information in order to avoid errors in the estimation of the number of layers. In the next section, we present results obtained on reference exfoliated samples deposited on soda lime glass and SiO_2/Si substrates. Additional limitations in the case of SiO_2/Si substrates are discussed. Finally, we present the proposed method for the specification of the number of layers based on the combination of Raman spectroscopy (normalized G-band area) and optical reflection (optical contrast) and specify its domain of validity.

2) Experimental methods

a) Samples preparation

The chemical vapor deposition (CVD) graphene flakes are synthesized at ambient pressure. The copper pieces (99.9% purity, 50 µm thick, 1 cm^2) are first deoxidized in acetic acid. Next, they are inserted into a quartz tube inside a hot wall furnace set at 1050 °C. During the first 30 minutes, only argon (Ar, 500 sccm) is flown to slightly oxidize the copper surface thanks to residual oxidizing impurities [41] (oxidative annealing [42,43]). During the next 30 minutes of annealing, hydrogen (H_2, 20 sccm) is introduced. Next, 0.4 sccm of methane (CH_4) diluted in Ar (with a 5:95 CH_4/Ar ratio) is added for 1 hour to grow isolated submillimeter graphene hexagonal domains. Finally, the quartz tube is manually extracted from the furnace for rapid cooling, still in the same gas mixture.

For the transfer, the copper sample is covered by a poly(methyl methacrylate) (PMMA) film baked at 80 °C for 15 min. Then, copper is etched in ammonium persulfate for few hours, then rinsed in distilled water, and transferred onto SiO_2/Si or soda lime glass substrates. In the end, the PMMA film is dissolved into acetone, the sample is rinsed in isopropanol, and blown-dry with nitrogen.

Graphene flakes were also prepared by mechanical exfoliation of SCG on soda lime glass or SiO_2/Si substrates using blue Nitto tape. Prior to exfoliation, the substrates were cleaned using solvents or in oxygen plasma to remove organic residues.

b) Raman, reflection, transmission setup

The scheme of the setup is presented on Figure 1. Raman spectra were recorded using an Acton SP2500 spectrometer fitted with a Pylon CCD detector and a grating that enables the measurement of the full spectrum in the range 1000-3000 cm^{-1} within a single acquisition (*i.e.* for a 532 nm laser, 600 grooves/mm grating corresponding to ~2 cm^{-1} between each CCD pixel). The samples were excited with a 532 nm (2.33 eV) laser (Millennia Prime, Newport) through 100x or 50x objectives (Numerical Aperture 0.9 and 0.5, respectively). Optimized focus conditions have been checked for each measurement. The samples are mounted on a three-axis piezoelectric stage (Physik Instrumente) to ensure the precise positioning and focusing of the laser spot. The maps (typically ~50000 points) were recorded with a 0.25 µm or a 0.2 µm step in both X and Y directions. The laser power was continuously measured by a calibrated photodiode put behind the beam splitter which enables to correct the laser power fluctuations during the sample mapping. To perform simultaneously microreflection (OC) (resp. microtransmission (optical extinction)) measurements and Raman spectroscopy, a low noise photodiode is placed on the path of the laser beam reflected by the edge filter located in front of the spectrometer's entrance slit (resp. under the sample). The laser OC, defined as previously by OC = (Rs-R)/Rs, where R (resp. Rs) is the reflected intensity of the 532 nm laser light measured on each point of the sample (resp. on the bare substrate). The whole experimental setup (spectrometer, piezoelectric stage, photodiodes…) was controlled by a dedicated, home-made Labview application. The acquisition time for each individual spectrum was adjusted to exceed a signal to noise ratio of 50 for the G band (with a 532 nm laser, 1 mW on the sample and a 100x objective, the requested acquisition time is 0.5 s (resp. 2 s) for graphene on SiO_2/Si (resp. glass)). Optical doping or de-doping can occur at such power [44], this would however not affect the conclusions drawn here since A_G is doping independent except for very high doping [45]. The experimental setup is fully enclosed to avoid any external perturbations. Together with its designed great mechanical and laser pointing stabilities, this allows to almost cancel any XYZ drifts typically due to ambient temperature changes. A home-made data analysis software was used to treat the ensemble of the data (including normalization of the intensity with regards to that of HOPG (reference sample), corrections of the laser fluctuations, background subtraction, fitting of the bands…).

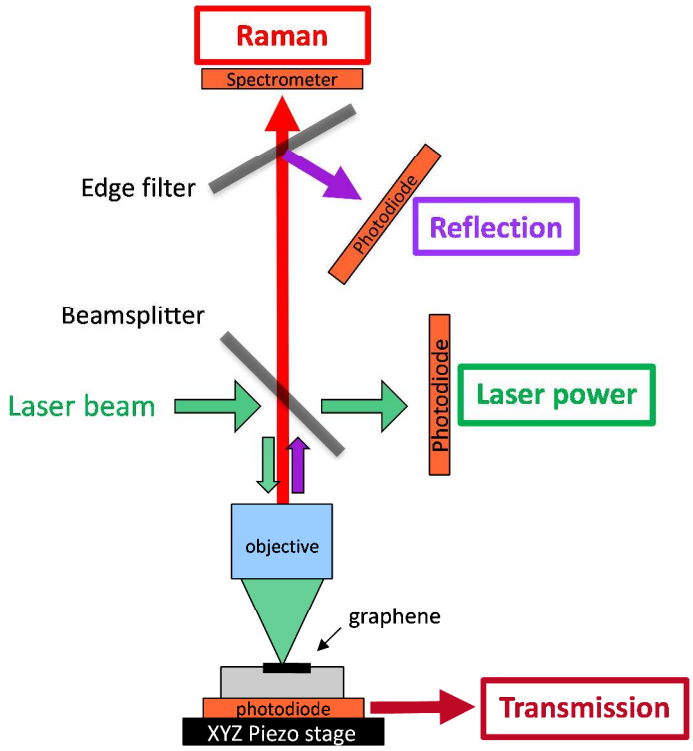

Figure 1: Scheme of the Raman/reflection/transmission setup.

3) Mechanically exfoliated FLG as reference

An example of extracted maps in the case of a mechanically exfoliated FLG sample (assigned as AB or ABC stacks) deposited on a 89 nm SiO_2/Si substrate is shown in Figure 2. In Figure 2a, the optical image of the mapped region is shown. The estimated SiO_2 thickness as well as the N labelled on Figure 2a were determined by the combination of spectral microreflection in the 400-800 nm range [28], Raman and laser OC. In Figure 2b (resp. 2c), the obtained A_G^{Norm} (resp. OC) map is shown. As evidenced by the profiles plotted in Figure 2d, both quantities show a clear, correlated dependence on N. These profiles also give an insight into the signal to noise ratio that can be obtained in this ideal case.

In the following, the results obtained on mechanically exfoliated FLG samples are used as reference. Raman and OC maps, as those presented in Figure 2, have been statistically analyzed and the obtained distributions of the measured A_G^{Norm} and OC have been fitted using Gaussian functions to obtain the average values for each N. The detailed dependencies of A_G^{Norm} and OC with N will be presented and discussed in the section 5. In the following section 4, we first discuss the limitations of the A_G and OC criteria related to the relative orientation and stacking of the graphene layers.

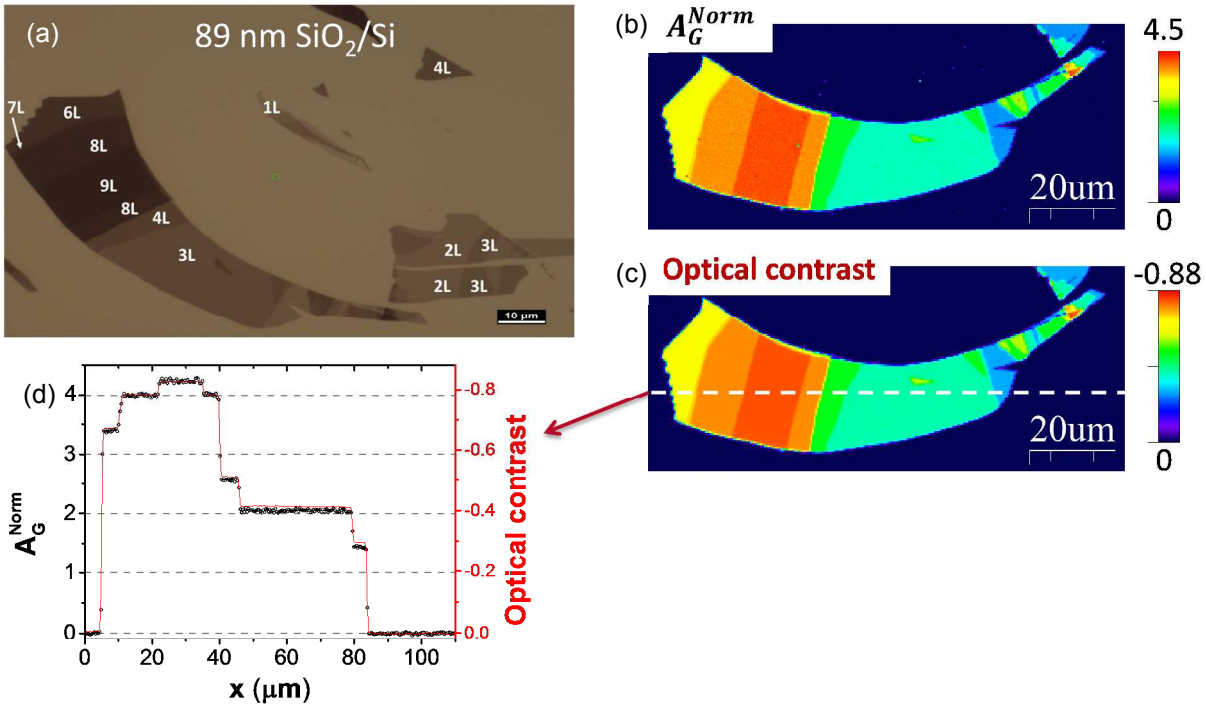

Figure 2: (a) Optical microscopy image of a FLG sample deposited by micromechanical exfoliation on 89 nm SiO_2/Si. The number of layers N is labelled as NL on the corresponding regions of the image and has been determined by spectral microreflection, Raman and laser optical contrast. (b) G band integrated intensity normalized versus the one of HOPG map and (c) Optical contrast map extracted from a Raman/reflection mapping of the sample with a 532 nm laser and a 100x objective. (d) Profile along the white dotted line on (c) of the A_G^{Norm} (left Y axis) and optical contrast (right Y axis).

4) Limitations related to the relative orientation and stacking of the graphene layers

a) First limitation: optical resonance in FLG

A_G and OC can be enhanced due to singularity(ies) in the joint density of states of twisted FLG, whose energy is a function of the relative twist angle between consecutive layers [39]. As exemplified in Figure 3b, for 2LG deposited on a suitable substrate, optical resonances falling in the visible range can lead to specific coloration on optical microscopy images [46]. Moreover, the OC is significantly enhanced in a wavelength range associated to a specific twist-angle, as evidenced in ref. [39] and exemplified in Figure 3c. Regarding A_G, the amplification effect is much more pronounced than for OC [21,22,33]. To illustrate this point, we discuss results obtained on twisted 2LG with different twist angles deposited on a 300 nm SiO_2/Si substrate and measured using a laser wavelength of 532 nm. The dependence of the laser OC and of A_G relative to the A_G of AB-2LG are plotted as a function of

the wavenumber of a peculiar mode, the so-called TO or R mode [47] (Figure 4a). The TO mode is activated in Raman spectroscopy by the rotational disorder (twist) between the layers and it was established that the wavenumber of the TO mode is directly related to the value of the twist angle [47]. The data presented in Figure 4a correspond to twist angles in the range 10° to 16° [47]. As shown in Figure 4a (top panel), the laser OC of the twisted 2LG around the optical resonance can slightly decrease (by about 30% for TO wavenumber around 1480 cm^{-1} in Figure 4a) or increase by a factor up to 2 depending on the twist angle and as compared to AB-2LG (for TO wavenumber around 1495 cm^{-1} in Figure 4a). By comparison with data obtained on AB-FLG deposited by mechanical exfoliation on the same substrate, the values of the laser OC of twisted 2LG ranges from 1.5 times that of 1LG up to that of AB-4LG. The effect on A_G is much more pronounced since its intensity can reach 50 times that of AB-2LG (Figure 4a bottom panel). In order to determine the impact of this on the determination of N using A_G and OC, the relation between the intensity of the G band and the value of OC near the resonance is shown in Figure 4b (green dots). The same quantities measured on exfoliated NLG (N≤4) are presented for comparison (Figure 4b, black circles). This plot illustrates that no point measured near the optical resonance of twisted FLG overlaps with the one measured on exfoliated (and assigned as AB or ABC stacks) FLG samples. Conversely, this means that if the A_G and OC values obtained on Bernal FLG are used to estimate the number of layers, N_G from A_G and N_{OC} from OC, N_G and N_{OC} will always be significantly different near resonance. In other words, the two criteria disagree and N cannot be determined by the proposed method. This highlights the need to measure both quantities to avoid errors. To conclude, in the optical resonance case, N cannot be determined reliably either using A_G or OC. Nevertheless, the method allows to identify that the estimated N is wrong and that the conclusion should be disregarded.

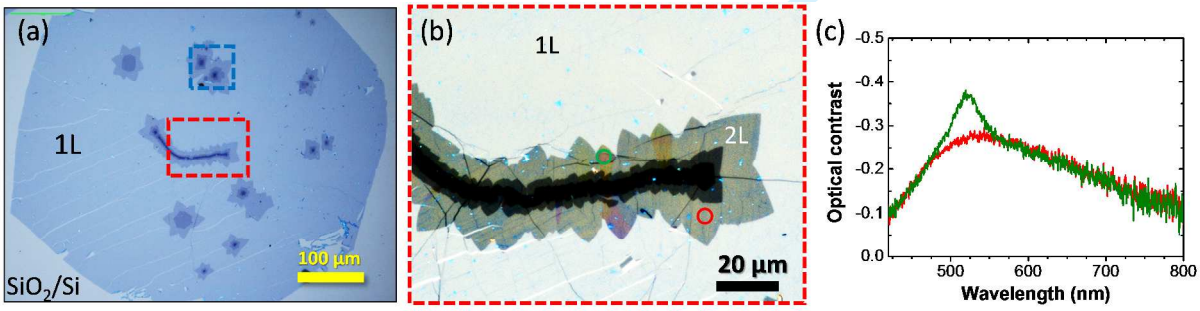

Figure 3: (a) Optical image of a single-layer graphene flake (1L) including multilayer patches (darker regions) synthesized by CVD on copper and transferred on a 90 nm SiO_2/Si substrate. (b) Optical image corresponding to a zoom in the region delimited by the red square in the low magnification image (a). The contrast of this image has been enhanced to make more evident the different colorations which are due to the angle-dependent electronic properties of t2LG [46]. Sharp blue regions correspond to PMMA residues from the transfer process. (c) Optical contrast spectra recorded in the regions delimited by circles in (b). The red (resp. green) spectrum corresponds to the red (resp. green) circle in (b).

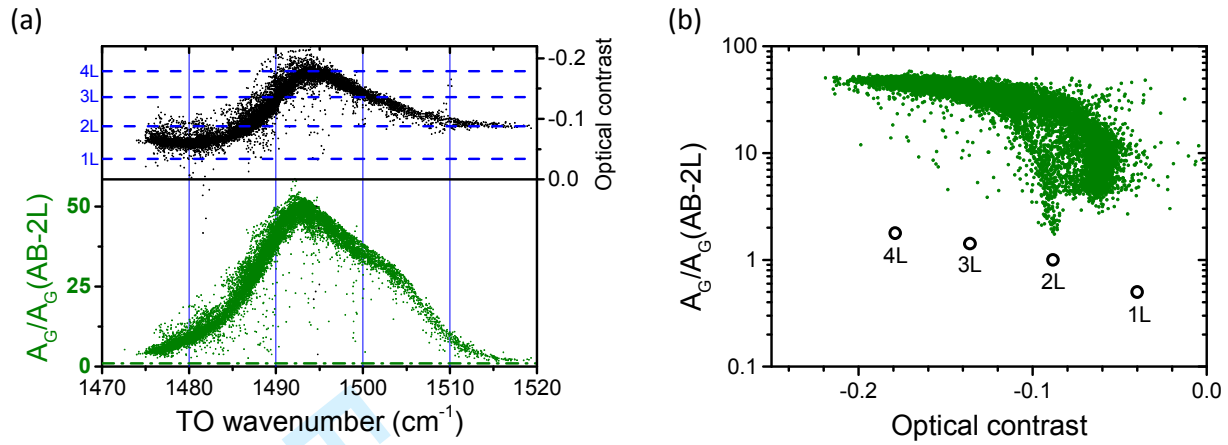

Figure 4: Illustration of the impact of an optical resonance for bilayer graphene (2L) deposited on 300 nm SiO_2/Si substrate. (a) top panel (black points) optical contrast and bottom panel (green points) A_G relative to the A_G of AB-2L as a function of the TO wavenumber (related to the twist angle between the two layers [47]) measured with a 532 nm laser. The horizontal blue dashed lines in the top panel represents optical contrast of mechanically exfoliated samples 1L to 4L as labelled on the figure. The horizontal green dot-dashed line in the bottom panel highlights the value 1. (b) A_G relative to the A_G of AB-2L as a function of the optical contrast. The green filled dots correspond to data presented in (a) and the black open circles correspond to data obtained on mechanically exfoliated samples (1L to 4L as labelled on the plot) deposited on an equivalent substrate.

b) Second limitation: lower G-band intensity in FLG

It has been reported that for some twist angles the A_G of 2LG and FLG can be less intense than that of Bernal stacked systems with an equivalent number of layers [34,35]. In order to illustrate this situation, maps recorded on the region delimited by the blue square in Figure 3a are displayed in Figure 5. The mapped region shows two distinct "flowers-like" domains close one to another defined as F1 and F2. In Figure 5a, the map of the laser OC is displayed. It allows to identify a single layer region (1LG, violet), and, in both "flowers", a large part of bilayer (2LG, dark blue) and different multilayer graphene regions (light blue to red as the number of layers increases). As discussed in Ref. [18], in the F1 (resp. F2) the twist angle between consecutive layers has been determined as smaller than ~8° (resp. larger than 20°). The important conclusion is that the measured laser OC (Figure 5a) for a given number of layers is equivalent on both "flowers" (see Ref. [18]), while this is not the case for A_G^{Norm} as shown on its map (Figure 5b). To get more insight into the distinct features of these two regions, we perform a statistical analysis of the maps displayed in Figures 5a and 5b and plot the 3D bivariate histograms corresponding to OC and A_G^{Norm} (Figure 5c). In this plot, high frequencies of occurrence are identified for distinct OC values which are ascribed to a given N (as shown on the top axis and by the vertical dashed blue lines in Figure 5c, see Ref. [18]). The data of the top (resp. bottom) curve have been measured on F1 (resp. F2). Outliers mainly correspond to frontiers between regions of different N, but also to ripples, residues, etc. For comparison, we also report in Figure 5c (black open circles) the dependence of A_G^{Norm} versus OC measured on mechanically exfoliated FLG assigned as AB or ABC stacks. These results clearly highlight

the fact that A_G^{Norm} is found slightly but significantly lower for FLG with large twist angles (F2) than for the ones with low twist angles (F1). Overall, we found during our investigations that this G-band intensity can drop down to 70% that of equivalent AB-stacked structures for some relative orientations (results not shown). On the other side, the laser OC remains unaffected in this case.

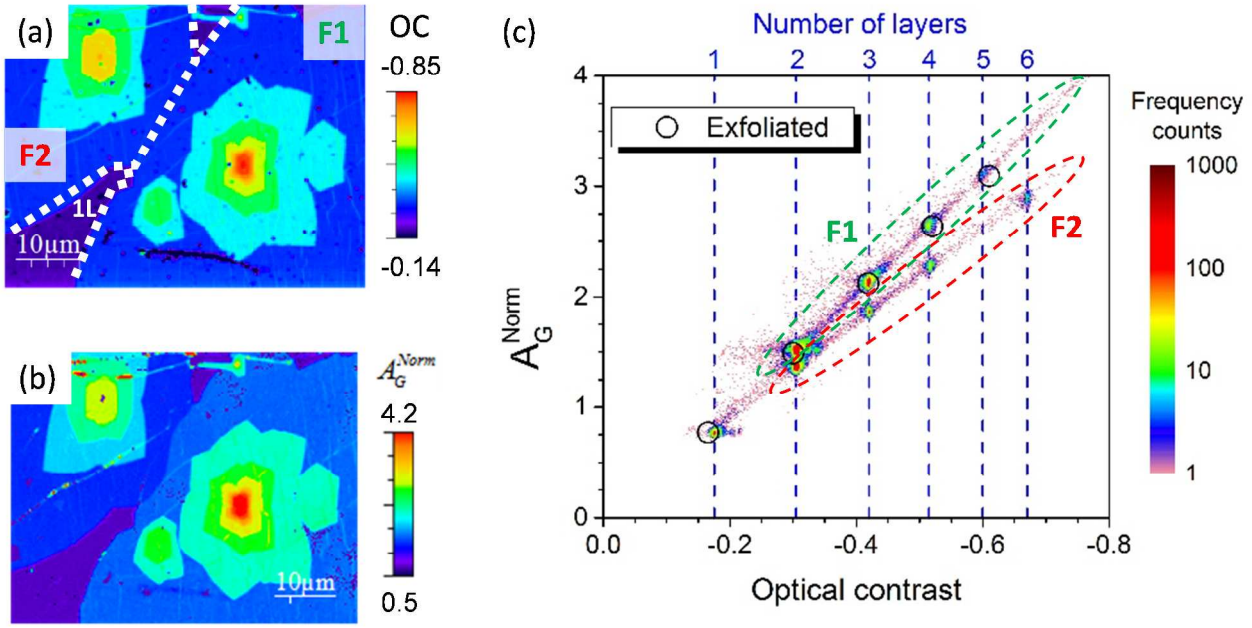

Figure 5: Illustration of the case where A_G^{Norm} is found lower than in equivalent Bernal stacked systems. (a) laser optical contrast and (b) G-band integrated intensity normalized versus the one of HOPG maps obtained on a sample made by CVD on copper and transferred on a 90 nm SiO_2/Si substrate (this region is located on the top of Figure 3(a) where it is delimited with a blue square, see also Figure 1 of ref. [18]). In (a), the 1L region is indicated and two distinct "flowers-like" domains labeled as F1 and F2 are separated by the dotted white line. (c) 3D bivariate histogram of A_G^{Norm} and laser optical contrast extracted from maps (a) and (b). The green (resp. red) dotted ellipse highlighted the data from region F1 (resp. F2) as labelled on the graph. The open circles are data obtained on mechanically exfoliated samples on 90 nm SiO_2/Si substrates. The corresponding number of layers is shown on the top axis and by the vertical dashed blue lines.

5) Method for the specification of the number of layers based on the combination of normalized G-band area and optical contrast

In this part, we discuss the possibility to define a reliable method for the specification of the number of layers, up to 5 layers, based on the combination of Raman spectroscopy (A_G^{Norm}) and optical reflection (OC). Both techniques enable, in controlled experimental conditions (laser power, focus, substrate, high signal to noise ratio…), to distinguish unambiguously between 1LG and multilayer graphene since the limitations discussed above do not affect the 1LG case. However, we have shown in the previous part that neither each method separately nor the combination of the two enable a determination of the number of

layers for all possible stacking orientations. But, the two methods always significantly disagree when they fail and this allows to define reliable criteria for counting N but not to count N in all possible cases. Indeed, by comparing the values deduced by each method it can be discriminated if the determined number of layers is correct and can be specified or not.

As a starting point, mechanically exfoliated samples are measured as reference samples with a well-defined stacking structure (AB or ABC), low defect density and low residue and the other cases discussed above are taken into account to define specification criteria. Two cases are discussed, FLG deposited on soda lime glass and on SiO_2/Si substrates. Each point in the following graphs represents statistical analysis of maps of thousands of measured points. The error bars are set at ± 3 sigma of the distribution of measured values and also include the error of the measured reference (of the order of 2% for A_G^{HOPG}).

a) Soda lime glass substrate

A_G^{Norm} and laser OC as a function of the number of layers measured on mechanically exfoliated samples on soda lime glass using a 532 nm laser and 100x objective (NA 0.9) are presented on Figure 6. The data are fitted using the relations:

$$N_G = 7.16 \times A_G^{Norm} + 3.36 \times \left(A_G^{Norm}\right)^2 \quad (1)$$

and

$$N_{OC} = 10.6 \times OC - 1.1 \times (OC)^2 \quad (2)$$

Where N_G and N_{OC} are the number of layers estimated from A_G^{Norm} and OC, respectively.

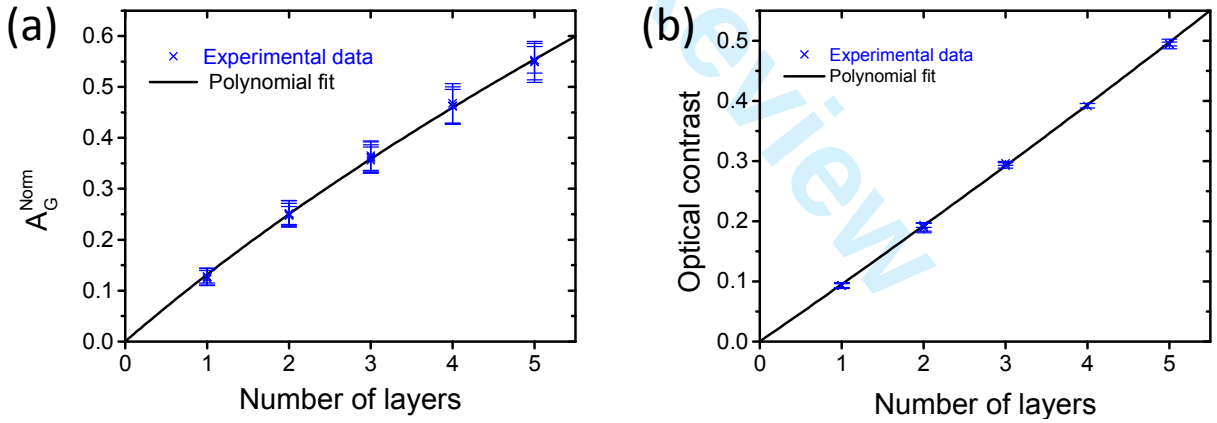

Figure 6: (a) A_G^{Norm} and (b) optical contrast as a function of the number of layers (N) measured on mechanically exfoliated samples on soda lime glass (blue dots). The solid black lines are the polynomial fits corresponding to eq. (1) and (2) in the text (coefficients of determination: R^2=0.9998 and R^2=0.9999 for A_G^{Norm} and optical contrast, respectively).

b) SiO_2/Si substrates

On SiO_2/Si substrates, additional limitations of the method have to be considered. Firstly, silicon wafer suppliers specify usually the thermal oxide (SiO_2) thickness at ± 5%. In this work, the precise SiO_2 thicknesses near the studied graphene/FLG flakes were measured using spectral microreflection. This method was validated using ellipsometry and transmission electron microscopy on specimens prepared by focused ion beam (not shown). Since 90 and 300 nm are the most used SiO_2 thicknesses as graphene substrate, we limit our discussion to these two cases although others have been investigated. We establish that the additional conditions necessary to ensure the reliability of the method for its application in different laboratories are:

(1) both A_G and OC should be close to their maxima in the specified SiO_2 thickness range to ensure a good accuracy of the measurements,

(2) A_G and OC values should exhibit weak variation with SiO_2 thickness in the 5% ranges,

(3) since the true NA of the microscope objective can vary for the incident laser light depending on the illumination conditions which can be different from one setup to another, it is also important that the measured values (A_G and OC) have a weak dependence on NA.

As an illustration, the A_G^{Norm} and OC of exfoliated 1LG for different SiO_2 thicknesses measured with a laser wavelength of 532 nm and using two microscope objectives are presented in Figure 7. These data show that the conditions listed above are fulfilled for 90 ± 5 nm SiO_2 thicknesses but cannot be fulfilled for 300 ± 15 nm SiO_2. A_G^{Norm} and OC have been also measured for other numbers of layers and laser wavelengths (not shown) but the conclusion remains the same. Furthermore, this conclusion is also supported by theoretical calculations of the dependence of A_G^{Norm} and OC on the SiO_2 thickness for different numbers of layers, laser wavelengths and objective NA as exemplified for 1LG and a laser wavelength of 532 nm on Figure 7. These theoretical calculations were performed within an approach close to the one of references [30,40]; their details are beyond the scope of this paper and will be discussed elsewhere [48]. As a consequence, the method's application is limited to SiO_2 on silicon with a SiO_2 thickness of 90 ± 5 nm and a laser wavelength of 532 nm.

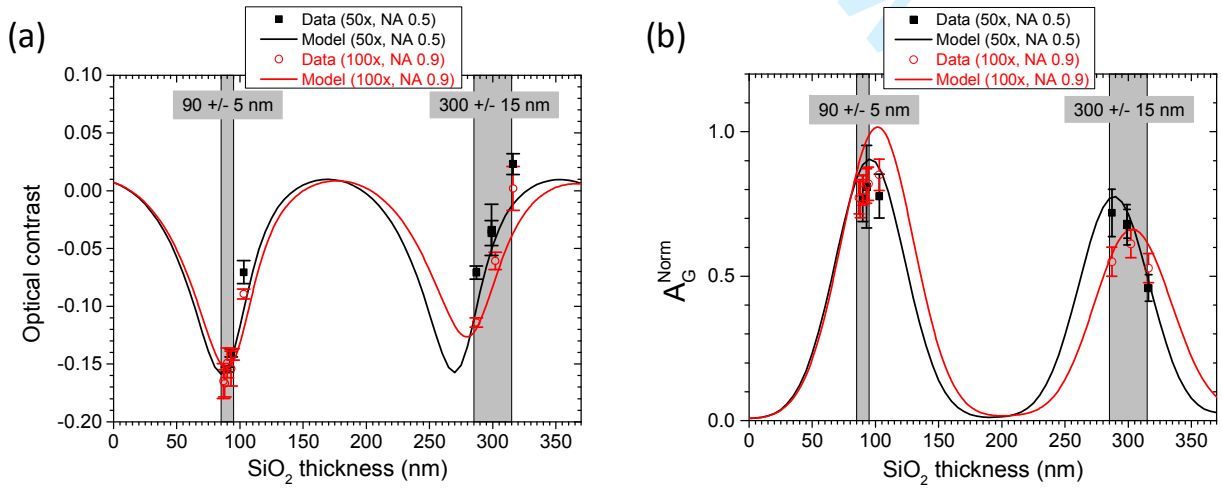

Figure 7: (a) Optical contrast and (b) A_G^{Norm} of 1LG as a function of the SiO_2 thickness for a 532 nm laser and two microscope objectives (50x, NA 0.5 (black) and 100x NA 0.9 (red)). Black squares and red open dots correspond to measurements, black and red lines to theoretical calculations [48]. The greyed regions highlight the 90 ± 5 nm and 300 ± 15 nm SiO_2 thickness ranges.

The A_G^{Norm} and laser OC as a function of the number of layers measured on mechanically exfoliated samples (5 to 10 for each N) on various 90 ± 5 nm SiO_2 on silicon substrates and using a 532 nm laser and 100x objective (NA 0.9) are presented in Figures 8a and 8b, respectively. The data are fitted using the relations:

$$N_G = 1.05 \times A_G^{Norm} + 0.16 \times \left(A_G^{Norm}\right)^2 \quad (3)$$

and

$$N_{OC} = -5.74 \times OC + 4.61 \times (OC)^2 \quad (4)$$

Additionally, the results of a round robin test conducted in two different laboratories (University of Montpellier and HORIBA) and using different spectrometers (Xplora at HORIBA) are also shown in Figure 9. The good agreement between the two sets of data constitute a first step towards the validation of the method using a standardization methodology.

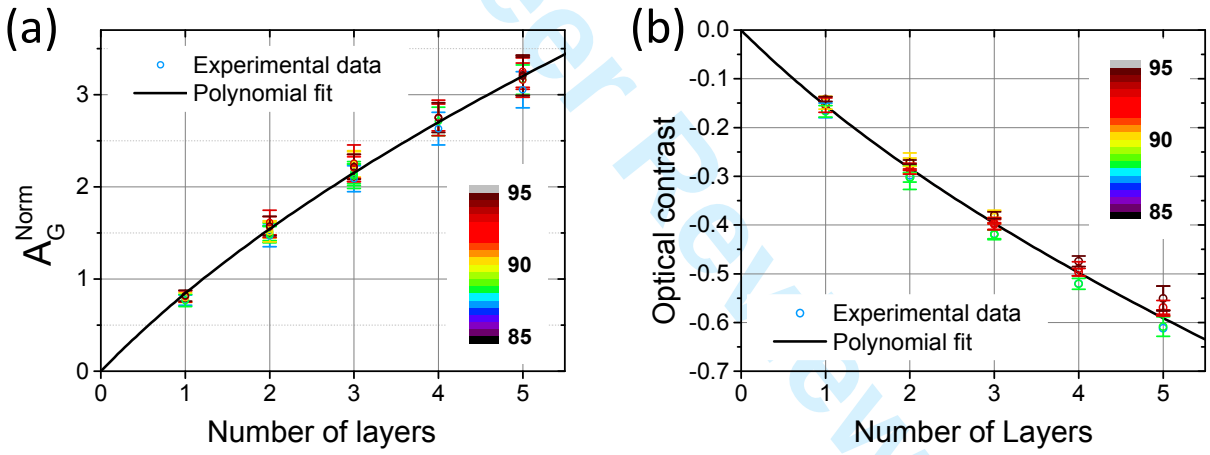

Figure 8: (a) A_G^{Norm} and (b) optical contrast as a function of the number of layers between 1 and 5 on 90 nm ± 5 nm SiO_2 on Si substrates. Open circles are experimental data (color coded with the SiO_2 thickness (nm) of the sample measured by spectral microreflection and as displayed on the graph) and the solid black line are polynomial fits corresponding to eq. (3) and (4) in the text (R^2=0.999 and 0.997 for A_G^{Norm} and optical contrast, respectively).

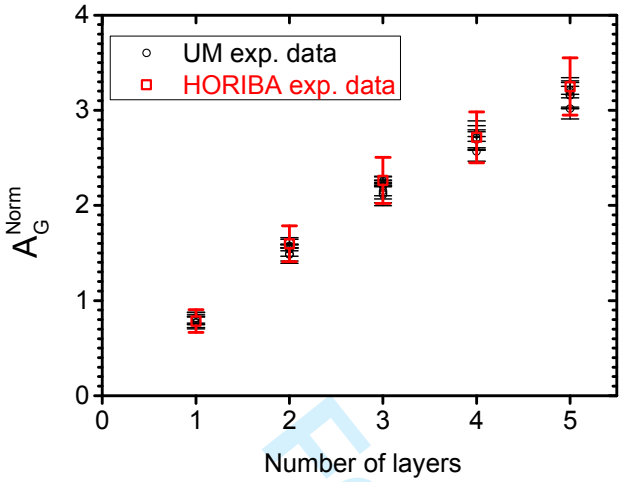

Figure 9: Comparison of the results obtained at University of Montpellier and at HORIBA for A_G^{Norm} as a function of the number of layers between 1 and 5 on 90 ± 5 nm SiO_2 on Si substrates and measured using a 532 nm laser wavelength and a 100x NA 0.9 objective.

c. Number of layers specification

To summarize, we provide a method to determine the number of layers for FLG on the following substrates: (i) glass (soda lime glass or similar with refractive index between 1.50 and 1.55) and (ii) oxidized silicon (SiO_2 on silicon, with a SiO_2 thickness of 90 ± 5 nm). The method is limited to high quality graphene and few layer graphene with small defect density and low residue and for a number of layers up to 5. The number of layers is determined by the combination of Raman spectroscopy and optical reflection. Criteria for the determination of the number of layers are the G-band normalized integrated intensity and the optical contrast measured with a 532 nm laser and using a 100x objective with a NA of 0.9. The obtained N_G and N_{OC} (using the relations (1) and (2) on glass and (3) and (4) on 90 ± 5 nm SiO_2 on Si) are two estimations of the number of layers with uncertainties related to the experimental errors and, more important, to the effect of stacking and optical resonance. The exact number of layers, N, can be obtained if N_G and N_{OC} agree with each other. The attribution of the number of layers from a set of data would then deserve to develop a full statistical analysis taking into account experimental uncertainties, and yielding number of layers likelihoods. This step still needs further developments and is beyond the scope of this paper. At this stage, we propose, as a first attempt, a graphical method using the values of N_G and N_{OC} (Figure 10). On this graph, which sketches the results discussed in this paper, the black and grey regions define in which cases N can be specified. The black regions correspond each to a given number of layers between zero and five while the grey regions correspond to non-integer numbers of layers and should be specified as: zero to one, one to two, etc. The cases where the method fails to give the true number of layers, *e.g.* when A_G^{Norm} or OC are influenced by an optical resonance, will fall out of the delimited region and N can be specified as larger than one and but not more precisely attributed.

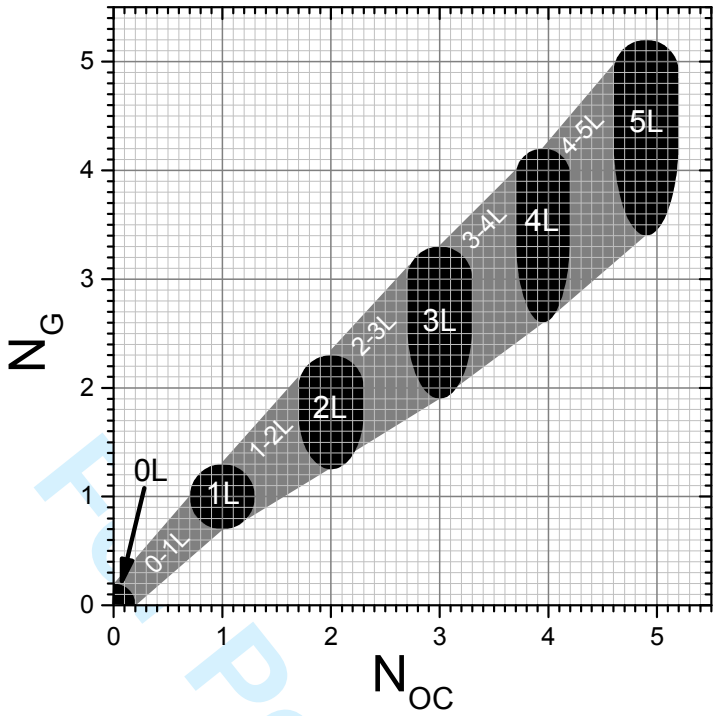

Figure 10: Schematic chart for the number of layers specification using the values N_G and N_{OC} determined from A_G^{Norm} and OC respectively, see text.

6) Conclusion

Combining simultaneous Raman spectroscopy and laser OC mapping, we discuss the use of the normalized G band integrated intensity (A_G^{Norm}) and of the laser OC for counting graphene layers in FLG samples. The Raman intensity normalization with an HOPG sample ensures the reproducibility and the transferability of the method on other equipment and in other laboratories. Beyond the Bernal stacked structures, we evidence different dependences of these two quantities as a function of the number of layers for some stacking order between consecutive graphene layers. As a consequence, we highlight the necessity to use both A_G^{Norm} and OC to avoid errors in the estimation of N. The exceptions related to the stacking angle do not affect the reliability of this method to distinguish between 1LG and FLG. However, neither each method separately nor the combination of the two enable a determination of the number of layers for all possible stacking orientations. Importantly, since the two methods always significantly disagree when they fail, the comparison of the values deduced by each method allows to discriminate if the determined number of layers is correct and can be specified or not. Finally, we were able to propose a reliable method for the determination of the number of layers for FLG deposited on the following substrates: (i) glass (soda lime glass or similar with refractive index between 1.50 and 1.55) and (ii) oxidized silicon (SiO_2 on silicon, with a SiO_2 thickness of 90 ± 5 nm). The method is limited to high quality

1LG and FLG with small defect density and low residue and for a number of layers up to 5. Criteria for the determination of the number of layers are A_G^{Norm} and OC measured with a 532 nm laser and using a 100x objective with a NA = 0.9.

Acknowledgements: The authors acknowledge Jean-Roch Huntzinger for his participation to this work and for providing the theoretical data. The authors acknowledge Raul Arenal for complementary experiments using FIB and TEM and helpful discussions and Norbert Fabricius for helpful discussions. This work was partly supported by the French ANR (Grafonics project ANR-10-NANO-0004) and has been done in the framework of the GDRI GNT 3217 “Graphene and Nanotubes: Science and Applications”. The research leading to these results have received partial funding from the European Union Seventh Framework Programme under grant agreement nº604391 Graphene Flagship and European Union Horizon 2020 research and innovation programme (EU Graphene Flagship grant agreement No. 696656). AF and JFC is supported by the Belgian fund for scientific research (FNRS).

References

[1] A.C. Ferrari *et al.*, *Nanoscale* **2015**, *7*, 4598.

[2] S. Latil, V. Meunier and L. Henrard, *Phys. Rev. B* **2007**, *76*, 201402.

[3] A.V. Rozhkova, A.O. Sboychakova, A.L. Rakhmanova and F. Nori, *Physics Reports* **2016**, *648*, 1.

[4] K.F. Mak, M.Y. Sfeir, J.A. Misewich and T.F. Heinz, *PNAS* **2010**, *107 (34)*, 14999.

[5] R. W. Havener, Y. Liang, L. Brown, L. Yang and J. Park, *Nano Lett.* **2014**, *14 (6)*, 3353.

[6] R. Sharma, J. H. Baik, C. J. Perera and M.S. Strano, *Nano Lett.* **2010**, *10 (2)*, 398.

[7] K.S. Novoselov, A.K. Geim, S.V. Morozov, D. Jiang, Y. Zhang, S.V. Dubonos, I.V. Grigorieva and A.A. Firsov, *Science* **2004**, *306*, 666.

[8] A.C. Ferrari, J.C. Meyer, V. Scardaci, C. Casiraghi, M. Lazzeri, F. Mauri, S. Piscanec, D. Jiang, K.S. Novoselov, S. Roth and A.K. Geim, *Phys. Rev. Lett.* **2006**, *97*, 187401.

[9] C.H. Lu, Z. Li, Z. Chen, P.V. Klimov, L.E. Brus and T.F. Heinz, *Nano Lett.* **2011**, *11 (1)*, 164.

[10] L. Brown, R. Hovden, P. Huang, M. Wojcik, D.A. Muller and J. Park, *Nano Lett.* **2012**, *12 (3)*, 1609.

[11] J. H. Warner, M.H. Rümmeli, T. Gemming, B. Büchner and G.A.D. Briggs, *Nano Lett.* **2009**, *9 (1)*, 102.

[12] X.-L. Li, W.-P. Han, J.-B. Wu, X.-F. Qiao, J. Zhang and P.-H. Tan, *Adv. Funct. Mater.* **2017**, 1604468.

[13] A. C. Ferrari and D. M. Basko, *Nat. Nanotech.* **2013**, *8*, 235.

[14] A. Bianco, H.-M. Cheng, T. Enoki, Y. Gogotsi, R.H. Hurt, N. Koratkar, T. Kyotani, M. Monthioux, C.R. Park, J.M.D. Tascon and J. Zhang, *Carbon* **2013**, *65*, 1.

[15] Mi.-L. Lin, T. Chen, W. Lu, P. Zhao, H.-T. Wang, Y. Xu and P.-H. Tan, this issue

[16] Mi.-L. Lin, T. Chen, W. Lu, P. Zhao, H.-T. Wang, Y. Xu and P.-H. Tan, this issue

[17] F. Herziger, P. May and J. Maultzsch, *Phys. Rev. B* **2012**, *85*, 235447.

[18] M. Bayle, N. Reckinger, J.-R. Huntzinger, A. Felten, A. Bakaraki, P. Landois, J.-F. Colomer, L. Henrard, A.-A. Zahab, J.-L. Sauvajol and M. Paillet, *Phys. Status Solidi B* **2015**, *252 (11)*, 2375.

[19] P. Poncharal A. Ayari, T. Michel and J.-L. Sauvajol, *Phys. Rev. B* **2008**, *78*, 113407.

[20] Z. Ni, Y. Wang, T. Yu, Y. You and Z. Shen, *Phys. Rev. B* **2008**, *77*, 235403.

[21] R.W. Havener, H. Zhuang, L. Brown, R.G. Hennig and J. Park, *Nano Lett.* **2012**, *12 (6)*, 3162.

[22] K. Kim, S. Coh, L.Z. Tan, W. Regan, J.M. Yuk, E. Chatterjee, M.F. Crommie, M.L. Cohen, S.G. Louie, and A. Zettl, *Phys. Rev. Lett.* **2012**, *108*, 246103.

[23] D.M. Basko, S. Piscanec and A.C. Ferrari *Phys. Rev. B* **2009**, *80*, 165413.

[24] R. Parret, M. Paillet, J.-R. Huntzinger, D. Nakabayashi, T. Michel, A. Tiberj, J.-L. Sauvajol and A.A. Zahab, *ACS Nano* **2013**, *7 (1)*, 16.

[25] C. Neumann, S. Reichardt, P. Venezuela, M. Drögeler, L. Banszerus, M. Schmitz, K. Watanabe, T. Taniguchi, F. Mauri, B. Beschoten, S. V. Rotkin and C. Stampfer, *Nat. Comm.* **2015**, *6*, 8429.

[26] A. Das, B. Chakraborty, S. Piscanec, S. Pisana, A.K. Sood and A.C. Ferrari, *Phys. Rev. B* **2009**, *79*, 155417.

[27] D. Graf, F. Molitor, K. Ensslin, C. Stampfer, A. Jungen, C. Hierold and L. Wirtz, *Nano Lett.* **2007**, *7*, 238.

[28] Z.H. Ni, H.M. Wang, J. Kasim, H.M. Fan, T. Yu, Y.H. Wu, Y.P. Feng and Z.X. Shen, *Nano Lett.* **2007**, *7 (9)*, 2758.

[29] Y.Y. Wang, Z.H. Ni, Z.X. Shen, H.M. Wang and Y.H. Wu, *Appl. Phys. Lett.* **2008**, *92*, 043121.

[30] P. Klar, E. Lidorikis, A. Eckmann, I.A. Verzhbitskiy, A.C. Ferrari and C. Casiraghi, *Phys. Rev. B* **2013**, *87*, 205435.

[31] X. L. Li, X. F. Qiao, W. P. Han, Y. Lu, Q. H. Tan, X. L. Liu, P. H. Tan, *Nanoscale* **2015**, *7*, 8135.

[32] Y. K. Koh, M. H. Bae, D. G. Cahill and E. Pop, *ACS Nano* **2011**, *5*, 269.

[33] J.-B. Wu, X. Zhang, M. Ijäs, W.-P. Han, X.-F. Qiao, X.-L. Li, D.-S. Jiang, A.C. Ferrari and P.-H. Tan, *Nat. Comm.* **2014**, *5*, 5309 and references therein.

[34] J.-S. Hwang, Y.-H. Lin, J.-Y. Hwang, R. Chang, S. Chattopadhyay, C.-J. Chen, P. Chen, H.-P. Chiang, T.-R. Tsai, L.-C. Chen and K.-H. Chen, *Nanotechnology* **2013**, *24*, 015702.

[35] H.B. Ribeiro, K. Sato, G.S.N. Eliel, E.A.T. de Souza, C.-C. Lu, P.-W. Chiu, R. Saito and M.A. Pimenta, *Carbon* **2015**, *90*, 138.

[36] C. Casiraghi, A. Hartschuh, E. Lidorikis, H. Qian, H. Harutyunyan, T. Gokus, K.S. Novoselov and A.C. Ferrari, *Nano Lett.* **2007**, *7 (9)*, 2711.

[37] P. Blake, E.W. Hill, A.H. Castro Neto, K.S. Novoselov, D. Jiang, R. Yang, T.J. Booth and A.K. Geim, *Appl. Phys. Lett.* **2007**, *91*, 063124.

[38] P.E. Gaskell, H.S. Skulason, C. Rodenchuk and T. Szkopek, *Appl. Phys. Lett.* **2009**, *94*, 143101.

[39] R.W. Havener, Y. Liang, L. Brown, L. Yang and J. Park, *Nano Lett.* **2014**, *14 (6)*, 3353.

[40] D. Yoon, H. Moon, Y.-W. Son, J.S. Choi, B.H. Park, Y.H. Cha, Y.D. Kim and H. Cheong, *Phys. Rev. B* **2009**, 80, 125422.

[41] N. Reckinger, X. Tang, F. Joucken, L. Lajaunie, R. Arenal, E. Dubois, B. Hackens, L. Henrard, and J.-F. Colomer, *Nanoscale* **2016** 8, 18751.

[42] H. Zhou, W.J. Yu, L. Liu, R. Cheng, Y. Chen, X. Huang, Y. Liu, Y. Wang, Y. Huang and X. Duan, *Nat. Comm.* **2013**, *4*, 2096.

[43] L. Gan and Z. Luo, *ACS Nano* **2013**, *7 (10)*, 9480.

[44] A. Tiberj, M. Rubio-Roy, M. Paillet, J.-R. Huntzinger, P. Landois, M. Mikolasek, S. Contreras, J.-L. Sauvajol, E. Dujardin and A.-A. Zahab, *Scientific Reports* **2013**, *3*, 2355.

[45] C.-F. Chen, C.-H. Park, B.W. Boudouris, J. Horng, B. Geng, C. Girit, A. Zettl, M.F. Crommie, R.A. Segalman, S.G. Louie and F. Wang, *Nature* **2011**, *471*, 617.

[46] J. Campos-Delgado, G. Algara-Siller, C. N. Santos, U. Kaiser and J.-P. Raskin, *Small* **2013**, *9 (19)*, 3247.

[47] J. Campos-Delgado, L.G. Cançado, C.A. Achete, A. Jorio and J.-P. Raskin, *Nano Res.* **2013**, *6*, 269.

[48] J.-R. Huntzinger private communication.